Surface Domains and Roughness of Polymer Gels Observed by Atomic Force Microscopy

A. Suzuki,* M. Yamazaki, Y. Kobiki, and H. Suzuki

Department of Materials Science, Yokohama National University, 79-5 Tokiwadai, Hodogaya-ku, Yokohama, 240 Japan

Received October 29, 1996; Revised Manuscript Received January 31, 1997[⊗]

ABSTRACT: The surface roughness of polymer gels was investigated by tapping mode atomic force microscopy (AFM). The spongelike domains on *N*-isopropylacrylamide (NIPA) gels were directly observed in water. It was found that the surface domain structure was strongly affected not only by the degree of the homogeneities of polymer networks but also by the bulk phase transition in response to the change in the external temperature. The domain size of homogeneous gels prepared at the ice temperature was found to be much smaller than that of the inhomogeneous gels prepared at a temperature above the cloud point of NIPA polymers. The surface structure was reproducibly observed at exactly the same position below and above the volume phase transition temperature, and its change was found to be reversible with temperature. The surface roughness due to the spongelike domains was discussed in terms of the autocorrelation function, the root-mean-square roughness, and the power spectral density, which were calculated from the AFM images.

Introduction

Polymer gels are made of cross-linked networks of polymers and liquids. It is well-known that such gels of simple composition can exist in two distinct phases, swollen and collapsed, in the liquid. Recently, we experimentally observed the microscopic domain structures on gel surfaces by contact mode atomic force microscopy (AFM) in the liquid solvent.[1] Changes of the domain structure have also been detected during the bulk volume phase transition.[2] The roughness due to the spongelike domains of the submicrometer scale was found to be strongly affected by the nature of the gel networks as well as environmental conditions. The qualitative properties of the surface structure of gels have been discussed on the basis of a hypothetical model of two-dimensional gels based on the Flory−Huggins theory. Not only the nanometer scale (molecular) structure but also the submicrometer scale structure of polymer gels in the solvent should have important roles in the macroscopic properties such as adhesion and surface tension.

In this paper, we report further details of the surface domain structures on poly(*N*-isopropylacrylamide) (NIPA) gels at the submicrometer scale and their change during the bulk volume phase transition between the swollen and collapsed states. We investigated, for the first time, the effect of the homogeneities of the networks[3] on the domain structure as well as the effect of the temperature change[4] by using tapping mode AFM in water.[5−7] This imaging mode is one of the most commonly used oscillatory AFM techniques, and its operation under small oscillation amplitudes eliminates the lateral forces exerted on the sample surface by the scanning tip: It can reduce unnecessary damage to the sample[7] and enhance the ability of imaging soft materials such as polymer gels, which are practically difficult to image with contact mode AFM. The semiquantitative data for the surface structure of NIPA gels and its response to the temperature change are presented with reference to the roughness analysis,[8−16] using the autocorrelation function calculated from the AFM images. We have established that the surface of a synthetic polymer gel may have spongelike domain structures with discrete boundaries and exhibit a roughness change in response to external stimuli.

Experimental Section

The gels are synthesized by free radical copolymerization reactions between two glass plates with a thin spacer (thickness is about 50 μm or less). One of the gel surfaces is chemically adhered on a glass plate by using Bind Silane (Pharmacia). The details of the sample preparation have been described elsewhere.[1] The base solution, similar to the standard mixture for NIPA gel,[4] is 7.8 g of purified NIPA (Kohjin), 133 mg of *N,N′*-methylenebis(acrylamide) (Wako), and 240 μL of *N,N,N′,N′*-tetramethylethylenediamine (Wako) dissolved in 100 g of water, stored at the gelation temperature. After nitrogen gas is bubbled through the solution, 40 mg of ammonium persulfate (Wako) is added to initiate the reaction. The gelation is carried out overnight for completion of the reaction process. After the gelation, one glass plate is carefully removed from the gel, thus forming a clamped disk gel on the other glass plate, which is subsequently immersed into a large amount of deionized, distilled water to wash away residual chemicals and unreacted monomers from the polymer networks. The sample gel on a glass plate is placed in a specially designed temperature-controllable sample cell (a thermostatically-controlled small bath) with water, and the temperature is regulated within ± 0.05 deg. The gels used were prepared from the same pregel solution at the ice temperature (designated as 0 °C-gel) and at 40 °C (designated as 40 °C-gel); thus the respective network structures should be quite homogeneous (transparent) and inhomogeneous (opaque),[3] because the NIPA polymer has the lower critical solution temperature and its cloud point at the present concentration is reported to be around 32 °C.[17] During the polymerization the polymers are first under the influence of thermal fluctuations, but after reaching the gel point these thermal fluctuations become frozen into the gel networks; therefore the network structures in the gels prepared at 0 and 40 °C (below and above the cloud point) should be totally different from each other. We have prepared several samples by the same method at different times and observed the surface structures of 0 °C and 40 °C-gels.

The microscopic image of the NIPA gel surface in water was determined by tapping mode AFM (Digital Instruments, NanoScope III) with a Nanoprobe of 200 μm length, and a pyramidal oxide-sharpened silicon nitride cantilever with a spring constant of 0.12 Nm^{-1}. The amplitudes of the drive signal applied to the cantilever oscillation are used in the range between 0.5 and 2 V (typically 1 V). The tapping frequencies

[⊗] Abstract published in *Advance ACS Abstracts,* April 1, 1997.

S0024-9297(96)01598-7 CCC: $14.00

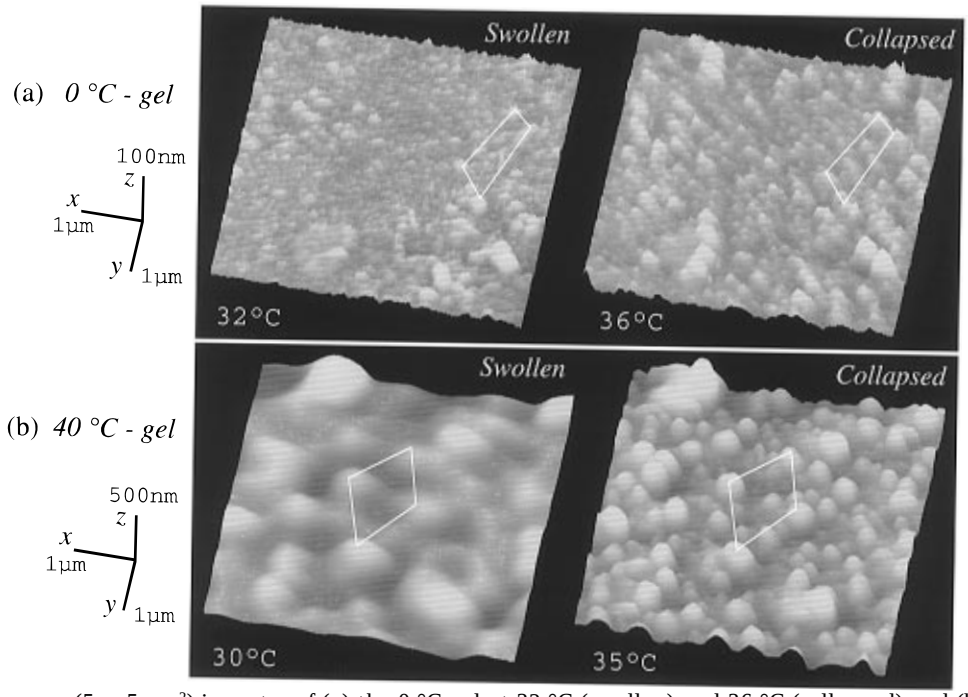

Figure 1. AFM images ($5 \times 5\ \mu m^2$) in water of (a) the 0 °C-gel at 32 °C (swollen) and 36 °C (collapsed) and (b) the 40 °C-gel at 30 °C (swollen) and 35 °C (collapsed). The vertical scales are greatly exaggerated to display clearly the spatial amplitude in the *z*-direction. Spongelike domains are visible in the submicrometer scale. The domains indicated by the tops of the white tetragonals correspond to the same domains.

ranged from 7.4 to 8.7 kHz, and the scan rates ranged from 0.8 to 1 Hz (typically 1 Hz). The images were processed only by flattening to remove background slope.

Results and Discussion

An equilibrium surface AFM image of 0 °C-gels, as pointed out in our previous study,[1] consists of undulations, large holes, and projections on the order of a few micrometers, among which there are flat regions. Figure 1 shows an example of the AFM images ($5 \times 5\ \mu m^2$) of the flat surface regions of the NIPA gels immersed in water with different homogeneities (the 0 °C-gel and 40 °C-gel) measured at a lower temperature (swollen phase) and a higher temperature (collapsed phase). The images were obtained at exactly the same position in each gel below and above the transition temperature (between 33 and 34 °C). As shown in these images, the overall conformations in the swollen and collapsed states of the 0 °C-gel were appreciably different from those of the 40 °C-gel: The amplitude as well as the width of the domains in the former are much smaller than those of the latter, while the total number of domains is much larger. Changes in the surface images below and above the transition temperature are clearly seen. This is particularly manifested in the 40 °C-gel. It should be noted that the changes were reversible as a function of temperature and could be imaged repeatedly without any damage caused by interaction with the probe tip. These observations on spongelike domains can quantitatively be expressed in terms of the autocorrelation function, $g(r)$, defined as

$$g(r) = \langle h(r_0)\, h(r_0+r)\rangle_{r_0} - {h_0}^2$$
$$= \langle (h(r_0) - h_0)(h(r_0+r) - h_0)\rangle_{r_0}$$

where $h(r_0)$ and $h(r_0+r)$ are the absolute values of height at position r_0 and $r_0 + r$, respectively, h_0 is the average of the values of height within the image (the number of data points is 256 × 256), and the angular brackets denote the average overall choices of the products. The

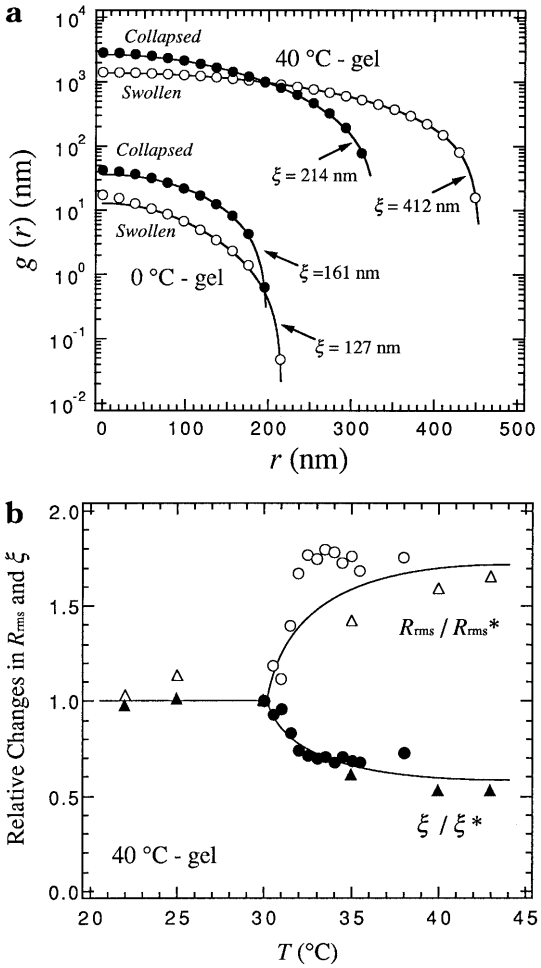

Figure 2. (a) Autocorrelation function, $g(r)$, of the AFM images in Figure 1. Open circles denote the respective swollen state, while closed circles the respective collapsed state. (b) Temperature dependence of R_{rms} and ξ at exactly the same position of the 40 °C-gels. Two examples indicated by circles and triangles from the different samples have been normalized by the values at 30 °C, R_{rms}*, and ξ*. There is a distinct correlation between R_{rms} and ξ.

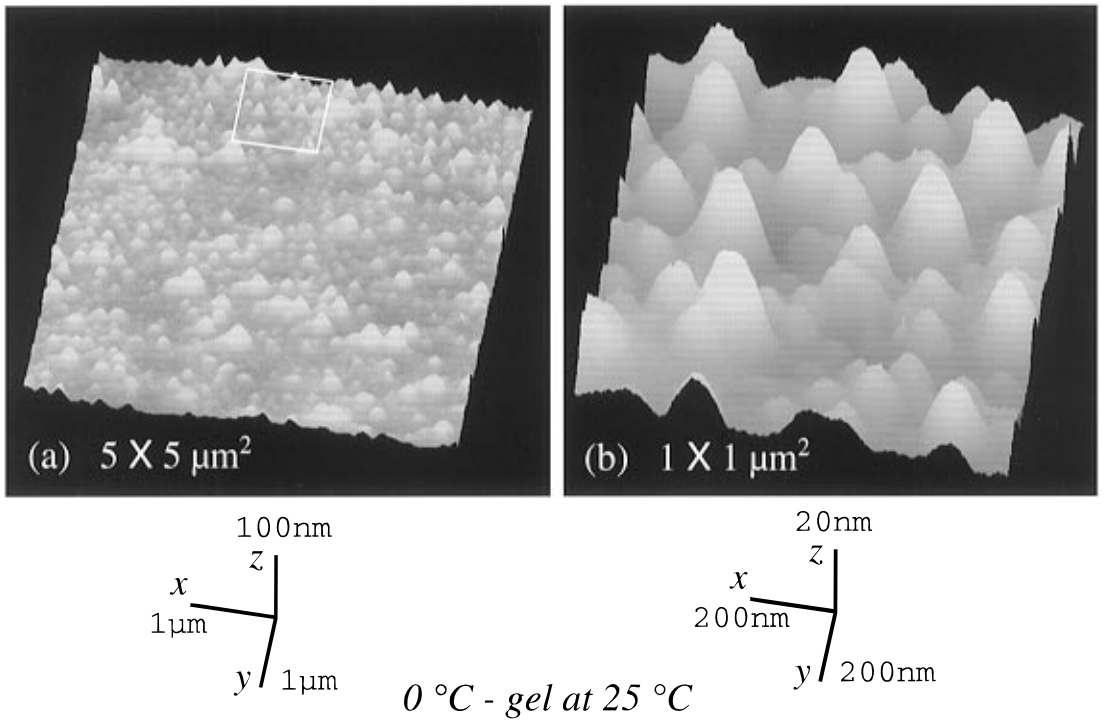

Figure 3. AFM images in water of the 0 °C-gel surfaces at 25 °C: (a) $5 \times 5\ \mu m^2$; (b) $1 \times 1\ \mu m^2$. The latter image is an example of a flat region that is obtained by scanning the $1 \times 1\ \mu m^2$ area surrounded by the white solid lines in the former one. The vertical scales have been greatly exaggerated to display clearly the spatial amplitude in the *z*-direction. Spongelike domains are clearly observed in this smaller size scale.

root-mean-square roughness R_{rms} is, therefore, equal to $g(0)^{1/2}$. We calculated $g(r)$ on the basis of the above equation by using the height values obtained from the AFM images (Figure 1). In Figure 2a, $g(r)$ is plotted as a function of r on a semilogarithmic scale. This figure indicates that all of the curves are basically parabolic in the range of $r < 200$ nm for the 0 °C-gel and of $r < 450$ nm for the 40 °C-gel. It was found that the values of $g(0)$ ($=R_{rms}^2$) of the 0 °C-gel were much smaller than those of the 40 °C-gel and that R_{rms} of the collapsed phase was larger than that of the swollen phase in each gel. If the surface is of perfect periodic wavelength, such as an artificial sinusoidal function, $g(r)$ should also be periodic. On the other hand, in a nonperiodic random surface, $g(r)$ rapidly decreases with increasing r, followed by a dumped oscillation. The topography of the random surface has been studied in many fields using statistical methods,[14,15] and several types of the decay function, $g(r)/R_{rms}^2 - g_0 \equiv f(r)$, have been reported,[8,12,16] where g_0 is a constant and corresponds to the incoherent background noise. The scaled decay function $f(r)$ satisfies the conditions that $f(r)$ goes to 1 as r goes to 0 and $f(r)$ goes to 0 as r goes to ∞. In the present system, we assume that the decay function may be expressed by a Gaussian function in the form $f(r) = \exp[-(r/\xi)^2]$, where r is small enough compared to the measured image size. The data points fit well to a Gaussian distribution, though a slight deviation could be observed for the 0 °C-gel in the range $r < 50$ nm, which will be discussed later. The observed image is characterized by a correlation length, ξ. It was found that the values of ξ of the 0 °C-gel are smaller than those of the 40 °C-gel, as presented in Figure 2a. In the case of the 40 °C-gel, we obtained $\xi = 412$ nm for the swollen state and $\xi = 214$ nm for the collapsed state: The surface domain size is uniform, then ξ is proportional to the characteristic domain size in each image. Now we can discuss the change in the domain size during the bulk volume phase transition on the basis of $f(r)$. Figure 2b presents the temperature dependence of the relative changes in R_{rms} and ξ at exactly the same position of each 40 °C-gel sample. It is obvious that both parameters, R_{rms} and ξ, which correspond to the topological feature of the characteristic domains, change noticeably below and above the transition temperature: With an increase of the temperature, R_{rms} exhibits a steep increase at around the transition temperature, which corresponds to the rapid decrease of ξ. The coincidence of the changes in both parameters can be regarded as resulting from the bulk volume phase transition due to rapid changes in the hydrophobic interactions between thermoresponsive polymer segments. The increase of R_{rms} may be attributed to the change in the balance of hydrophilic and hydrophobic interactions during the volume phase transition. Specifically, if the surface is relatively more hydrophobic, the surface free energy is lowered in the NIPA gel,[18,19] and therefore, the surface area might be maximized. This leads to formation of rough surfaces. The surface roughness might be determined by the competition between the thermal fluctuation and the surface free energy. It should be noted that the absolute values of R_{rms} and ξ obtained for several 40 °C-gel samples were not exactly the same, even though the relative change in each parameter with temperature does not depend on sample and its sampling region.

In the case of the 0 °C-gel, the image of the collapsed surface contains a greater number of larger peaks than that of the swollen surface (consistent with the R_{rms} increase with increasing temperature); however, the change in ξ and the number of domains show sample dependence and do not necessarily change noticeably below and above the transition temperature. Although ξ obtained from the image shown in Figure 1a slightly increases during the swollen to collapsed phase transition, it decreases slightly or does not change for other samples. This is because the deviation of the surface domain size is not small and the surface is composed of domains with different characteristic sizes. In fact, the characteristic length, ξ, that was obtained from the 5

$\times$ 5 μm^2 image, as well as its change from 127 to 161 nm, seems to be proportional to some domains but not to others. In order to interpret the image of the 0 °C-gel and its characteristic domain, it is necessary to measure the surface image at a higher magnification where the domain size is uniform. Accordingly, we observed several images of different magnifications from a specific 5 $\times$ 5 μm^2 image. Figure 3 shows such an example: First we obtained a 5 $\times$ 5 μm^2 image of a 0 °C-gel observed at 25 °C (Figure 3a). Compared to the image shown in Figure 1a, the mean size of the domains is slightly larger, which should be enhanced by the positive osmotic pressure at a lower temperature.[1] A flat region of the uniform size domains with 1 $\times$ 1 μm^2 scale was measured from the 5 $\times$ 5 μm^2 image (Figure 3b). As is shown in this image, spongelike domains with uniform sizes are clearly observed at this scan scale, the typical domain size is not small compared with the measured image size, and the image is very similar to that reported in ref 1. We calculated $g(r)$ from the AFM images (Figure 3) by the same method aforementioned. As shown in Figure 4a, $g(r)$ of the 1 $\times$ 1 μm^2 image is expressed by a single Gaussian function with ξ = 63 nm, while $g(r)$ of the 5 $\times$ 5 μm^2 image is not simply expressed by a simple function but can be deconvoluted to some components. We assumed that the 5 $\times$ 5 μm^2 image is composed of two kinds of domains, that is, the larger and smaller ones with $g_1(r)$ and $g_2(r)$, respectively. If the correlation between them is disregarded, the total $g(r)$ can be expressed as the sum of each correlation function. As is presented in the figure, the data points in the range r > 146 nm (=r_C) can be expressed by a Gaussian function, $g_1(r)$, with ξ_1 = 259 nm. Extrapolating $g_1(r)$ to the region where $r < r_C$ and subtracting it from the experimental data in this range can also be well expressed by another Gaussian function, $g_2(r)$, with ξ_2 = 75 nm. It should be noted that ξ_2, that is, one-third of ξ_1, is comparable to the characteristic domain size (ξ_2 = 63 nm) observed in the 1 $\times$ 1 μm^2 image (Figure 3b). Although the absolute values of the domain sizes slightly depend on the sample and its sampling region, the 5 $\times$ 5 μm^2 image of 0 °C-gels was found to be characterized by two correlation lengths, and the smaller length corresponds to the domain size dominated in the 1 $\times$ 1 μm^2 image.

From the general properties of $g(r)$, we can infer the corresponding properties of the power spectral density, $P_{PSD}(q)$, that is, the square of the magnitude of the Fourier transform of the autocorrelation function for any random field.[8−12] According to a general scaling description, $P_{PSD}(q)$ can be expressed as a scaling function of power-law behavior.[16] For the large scale of millimeter size, the surface can be considered to be flat, while for the smallest limit it should be reflected by the random chain structure. As for the intermediate size scale from 10 nm to 1 μm, the surface structure should depend on the characteristic domain size in the observed area. For this real-space behavior, one would expect that $P_{PSD}(q)$ should not depend on q as long as q is small enough, while it should decrease toward zero when q exceeds the inverse of the characteristic length of the surface. In Figure 4b, $P_{PSD}(q)$ is plotted as a function of the spatial frequency, q, in log−log scale, which was calculated from the AFM image in Figure 3. It is clearly observed that there are three linear relationships divided by two characteristic frequencies. The crossover frequencies were nearly equal to ξ_1^{-1} and ξ_2^{-1}. The observed linear behavior might be related to the surface dimensionality in the scale range from 10 nm to 1 μm: The surface structure exhibits the scaling behavior for

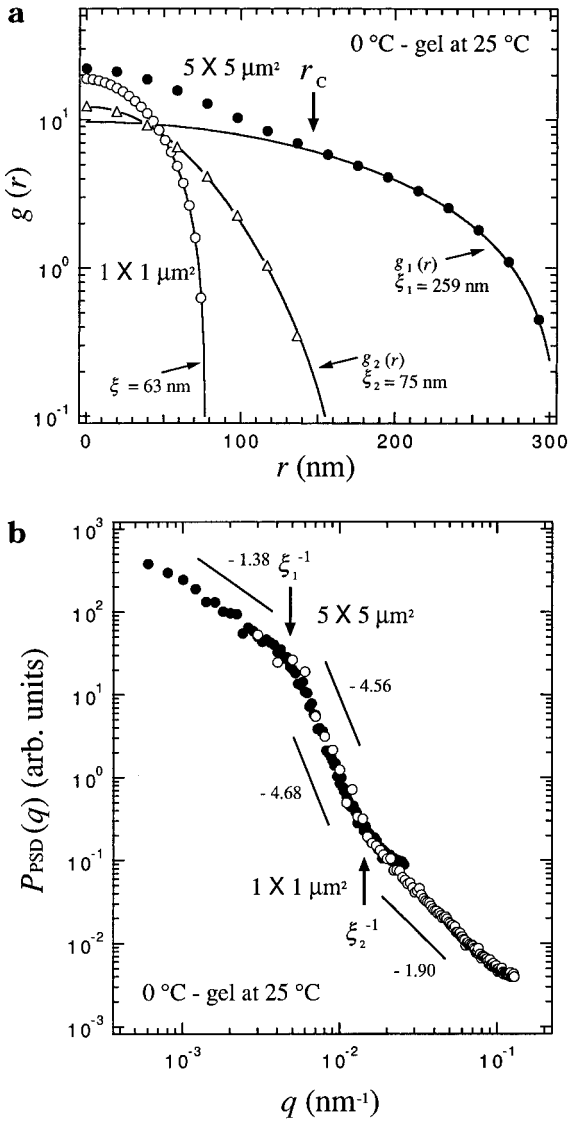

Figure 4. (a) Autocorrelation functions of the AFM images in Figure 3. Closed circles are from the 5 $\times$ 5 μm^2 image. The data in the range of $r > r_C$ have been fitted by a Gaussian ($g_1(r)$, solid line). Open circles are from the 1 $\times$ 1 μm^2 image and have been fitted by a Gaussian (solid line). Open triangles are obtained by subtracting $g_1(r)$ from the data of the 5 $\times$ 5 μm^2 image, which were also fitted by a Gaussian ($g_2(r)$, solid line). (b) Surface power spectral density as a function of spatial frequency calculated from the autocorrelation functions in (a), where the symbols are same as those in (a).

$q < \xi_1^{-1}$ due to the larger domain, but for $q > \xi_2^{-1}$ due to the smaller domain. Though we do not have a quantitative model to explain the characteristic length at this moment, the concept of power spectral analysis is very useful in the study of the surface topography of polymer gels in water. In order to develop such a model to explain the scaling behavior, it is important to observe different scan sizes as well as to measure the surface structures at different temperatures.

Conclusion

The surface structure and roughness of homogeneous and inhomogeneous NIPA gels prepared at different temperatures were investigated by using tapping mode AFM in water. The images were obtained at exactly the same position below and above the phase transition temperature. The surface structure and roughness of NIPA gels depend not only on the preparation temperature (below or above the cloud point of the NIPA polymers) but also on the state of the gels (swollen or

collapsed phase). The surface roughness changes with temperature corresponding to the macroscopic volume phase transition. Since the change in the domain structure is reversible with temperature, it is indeed an equilibrium roughness change due to the bulk phase transition. The surface domains and roughness of NIPA gels were characterized by the autocorrelation function, $g(r)$, R_{rms}, and ξ calculated from the AFM images. We believe that the present method is generally applicable and that the surface structures of polymer gels in the intermediate size scale can be elucidated by using tapping mode AFM in water.

Acknowledgment. We wish to thank Drs. T. Tanaka, M. Tokita, Y. Hirokawa, M. Annaka, and T. Tokuhiro for stimulating discussions. This work was supported by a SCF Grant from the Science and Technology Agency in Japan, by a Grant from the Ministry of Education, Science, and Culture in Japan, and by a Grant from the Nestle Science Foundation in Japan.

References and Notes

(1) Suzuki, A.; Yamazaki, M.; Kobiki, Y. *J. Chem. Phys.* **1996**, *104*, 1751.
(2) Tanaka, T. *Phys. Rev. Lett.* **1978**, *40*, 820.
(3) Matsuo, E. S.; Orkisz, M.; Sun, S.-T.; Li, Y.; Tanaka, T. *Macromolecules* **1994**, *27*, 6791.
(4) Hirokawa, Y.; Tanaka, T. *J. Chem. Phys.* **1984**, *81*, 6379.
(5) Binning, G.; Quate, C. F.; Gerber, C. *Phys. Rev. Lett.* **1986**, *56*, 930.
(6) Drake, B.; Prater, C. B.; Weisenhorn, A. L.; Gould, S. A.; Albrecht, T. R.; Quate, C. F.; Cannell, D. S.; Hansma, H. G.; Hansma, P. K. *Science* **1989**, *243*, 1586.
(7) Hansma, H. G.; Laney, D. E.; Bezanilla, M.; Sinsheimer, R. L.; Hansma, P. K. *J. Biophys.* **1995**, *68*, 1672.
(8) Rasigni, G.; Rasigni, M.; Varnier, F.; Palmari, J.; Palmari, J. P.; Llebaria, A. *Surf. Sci.* **1985**, *162*, 985.
(9) Wang, P.-z.; Howard, J.; Lin, J.-S. *Phys. Rev. Lett.* **1986**, *57*, 637.
(10) Eklund, E. A.; Bruinsma, R.; Rudnick, J.; Williams, R. S. *Phys. Rev. Lett.* **1991**, *67*, 1759.
(11) Iwasaki, H.; Yoshinobu, T. *Phys. Rev.* B **1993**, *48*, 8282.
(12) Brown, S. R.; Scholz, C. H. *J. Geophys. Res.* **1985**, *90*, 12575.
(13) Lifshitz, Y.; Lempert, G. D.; Grossman, E. *Phys. Rev. Lett.* **1994**, *72*, 2753.
(14) Yan, H.; Kessler, D.; Sander, L. M. *Phys. Rev. Lett.* **1990**, *64*, 926.
(15) Wang, X.-S.; Goldberg, J. L.; Bartelt, N. C.; Einstein, T. L.; Williams, E. D. *Phys. Rev. Lett.* **1990**, *65*, 2430.
(16) Thomas, T. R. *Rough Surfaces*; Longman: New York, 1982.
(17) Heskins, M.; Guillet, J. E. *J. Macromol. Sci.-Chem.* **1968**, *A2*, 1441.
(18) Zhang, J.; Pelton, R.; Deng, Y. *Langmuir* **1995**, *11*, 2301.
(19) Nakamura, T.; Hattori, M.; Kawasaki, H.; Miyamoto, K.; Tokita, M.; Komai, T. *Phys. Rev.* **1996**, *E54*, 1663.

MA961598R